

1 Introduction

The mechanical modelling of the behaviour of materials subject to large strain is a concern in a number of engineering applications. During deformation, the material may remain in the elastic range, as, for instance, when a rubber band is stretched, but usually inelasticity is involved, as, for instance, when a metal staple is bent. The achievement of severe deformations involves the possibility of the nucleation and development of non-trivial deformation modes—including localized deformations, shear bands and fractures—, emerging from nearly uniform fields. The description of the conditions in which these modes may appear, which can be analysed through bifurcation and stability theory, represents the key for the understanding of failure of materials and for the design of structural elements working under extreme conditions. Bifurcation and instability modes occur in a variety of geometrical forms (as can be shown with the example of a cylinder subject to axial compression) and may explain the so-called ‘size effect’, ‘softening’ and ‘snap-back’ even when fracture, damage and inelasticity are excluded. Shear banding can occur as an isolated event, leading to global failure, or as a repetitive mechanism of strain ‘accumulation’ (as can be shown through the examples of chains with softening elements). Features determining bifurcation loadings and modes strongly depend on the constitutive features of the materials involved (as can be shown with the example of the Shanley model for inelastic column buckling). The most general framework for inelastic behaviour, including metal plasticity as a particular case, is the so-called ‘non-associative elastoplasticity’, which permits the description of solids where Coulomb friction is the essential inelastic micromechanism, such as granular and rock-like materials. Within this framework, the perturbative approach to material instability is presented as a way to open new perspectives in the understanding of failure in ductile materials to explain, for instance, flutter instability, a form of dynamical instability related to the presence of dry friction (as will be demonstrated with a simple experiment). Final examples are included with the purpose of presenting the complete solution of a non-linear problem of elastic bifurcation and instability, the Euler elastica, and to show different features of instability (occurring for tensile dead loading and leading to multiple bifurcations or being suppressed when the load is proportionally increased from an unstable situation).

1.1 Bifurcation and instability to explain pattern formation

An initially flat and uniform surface of mud (Fig. 1.1, *top*) or of painting (Fig. 1.1, *centre*) has deformed under the effect of uniform drying (environmental exposition), initially undergoing a homogeneous deformation and eventually suffering a highly localized deformation, later evolving into a regular crack pattern. A presumably uniform mass of melt meteor iron has cooled down, giving rise to highly inhomogeneous but regular separation of different iron/nickel phases (so-called Widmanstätten pattern; Fig. 1.1, *bottom*). A common feature of these examples is that an initially homogeneous deformation field evolves, eventually self-organizing into an inhomogeneous but still regular deformation pattern. This phenomenon can be explained in different ways. One is to invoke the unavoidable lack of initial homogeneity of the materials into consideration, which, at least at an appropriate scale, must contain randomly distributed defects (an approach which in itself can hardly explain the regularity of the observed crack patterns). We are especially interested in another explanation,¹ which is in terms of bifurcation and instability theory so that the initial homogeneous deformation pattern (called ‘trivial’) ceases at a certain load level to be unique and stable, setting a bifurcation point in the deformation path and leading to an inhomogeneous alternative deformation pattern. Bifurcated deformation modes break the initially high-rank symmetry of the mechanical fields, thus introducing a lower-rank symmetry deformation pattern. The most famous example of bifurcation is Euler beam buckling (see Fig. 1.2*a*, where straight beams—with different constraints at the edges—have deformed, remaining initially straight under compressive loads but evolving into bent configurations after buckling).

Euler beam buckling (explained in Section 1.13.1) is a simple example of *elastic bifurcation and instability*: elastic because the beams in Fig. 1.2 immediately return to their initially straight configuration when the load is removed (so that permanent or viscous deformation is not involved), bifurcation because in the load/end-rotation diagram (Fig. 1.2*c*) the trivial equilibrium path corresponding to pure axial load bifurcates when the solution loses its uniqueness, and ‘instability’ because the straight configuration cannot be maintained after the first bifurcation load (while among the bent configurations only that corresponding to the first mode and for $\alpha < 130.7099^\circ$ is stable; see Section 1.13.1 for details) in the sense that an arbitrary small disturbance can induce a departure from the trivial configuration. Note that instability and bifurcation are different concepts, so a system can become unstable and still have a unique response to load.

Bifurcation also may involve irreversible deformation and thus be *plastic*, as is the case reported in Fig. 1.2*b*, where a steel specimen has been permanently deformed after loading in compression, and in Figs. 1.3 and 1.4, where rock layers subject to longitudinal compressive stresses have bifurcated and deformed in the plastic regime (see also Biot, 1965, and Price and Cosgrove, 1990).

¹ The dichotomy between the two approaches can be reconciled at least in part through the perturbative approach to material instability, which will be discussed later in this Introduction and detailed in Chapter 16, where a random distribution of dislocation-like defects is shown to induce regular deformation patterns in a metallic material pre-stressed near an instability threshold.

1.1 Bifurcation and instability to explain pattern formation

3

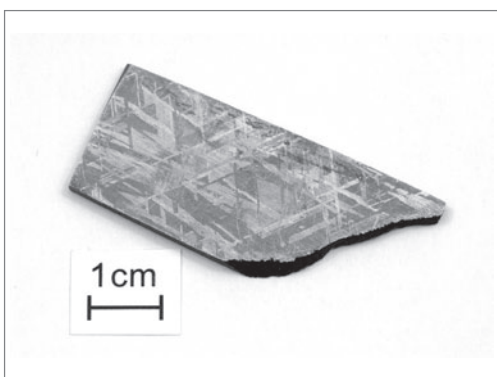


Figure 1.1. Pattern formation in initially uniformly deformed materials. *Top*: Regular crack patterns originated from drying of mud at Yaxha Lake, Petén Region, Guatemala. *Centre*: Regular crack patterns in a detail of a painting by Hieronymus Bosch (Bois-le-Duc 1450, Bois-le-Duc 1516) *La Crucifixion* (Musées Royaux des Beaux-Arts, Bruxelles). *Bottom*: A polished and etched section of an iron meteorite (a piece of the Gibeon meteorite, Namibian desert, purchased at a mineral exhibition in Trento, Italy) showing a Widmanstätten pattern. This is made up of alternate bands of kamacite (iron with 5% nickel) and taenite (iron with at least 13% nickel) developing during a cooling down process which may take thousands of years.

The fundamental difference between elastic and plastic bifurcation is that plastic deformation introduces a dissipative behaviour in the system so that the work performed to reach a certain final strain depends on the path involved (see the

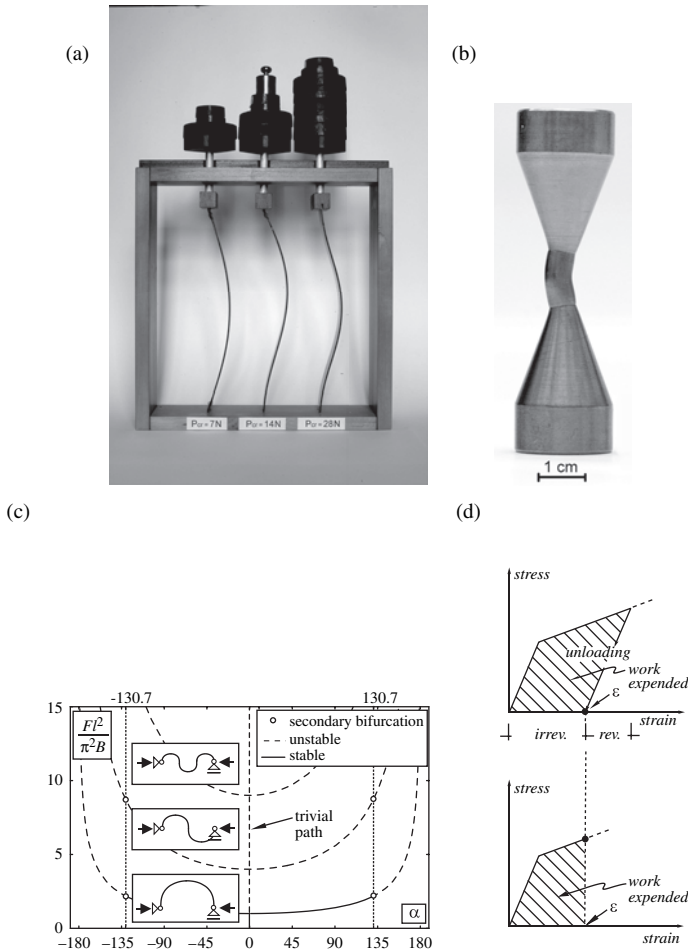


Figure 1.2. (a) Teaching model for buckling of beams with different end constraints (from left to right: hinged/hinged, hinged/clamped, clamped/clamped). (b) A metal sample subject to compressive load has buckled in the plastic range so that it is now permanently deformed. (c) The load (F normalized through division by π^2 times the bending stiffness B and multiplication by the square of the beam length l) versus end rotation (α in degrees) for a doubly supported inextensible Euler beam, evidencing the so-called ‘pitchfork’ diagram, with the ‘trivial’ and ‘bifurcated’ paths. Three bifurcation curves are shown, corresponding to the modes sketched. Note that all bifurcated paths superior to the first are unstable and that the first becomes unstable when the two supports of the beam coincide, corresponding to $\alpha = 130.7099^\circ$ and $F l^2 / (\pi B) = 2.1834$ (details can be found in Section 1.13.1). (d) A uniaxial stress/strain diagram for a plastic material evidencing irreversible deformation on unloading. This material defines a dissipative system; in fact, the work performed to reach, for instance, the final deformation ϵ is path-dependent.

example reported in Fig. 1.2d).² Other examples of plastic bifurcation are the bar-reeling of the initially cylindrical soil sample shown in Fig. 1.5 and the necking formed

² Dissipative terms also can be connected to the way in which the external loads are applied. For simplicity, we will always refer to conservative external load (dead loads or prescribed nominal tractions), whereas nonconservative loads are never considered in this book, with the exception of the the example on flutter instability (see the Exercise 1.13.5).

1.1 Bifurcation and instability to explain pattern formation

5



Figure 1.3. Gently folded rock layers (Silurian formation) at Constitution Hill, Aberystwyth, S. Wales, UK. The bending has been the consequence of buckling of initially straight layers.

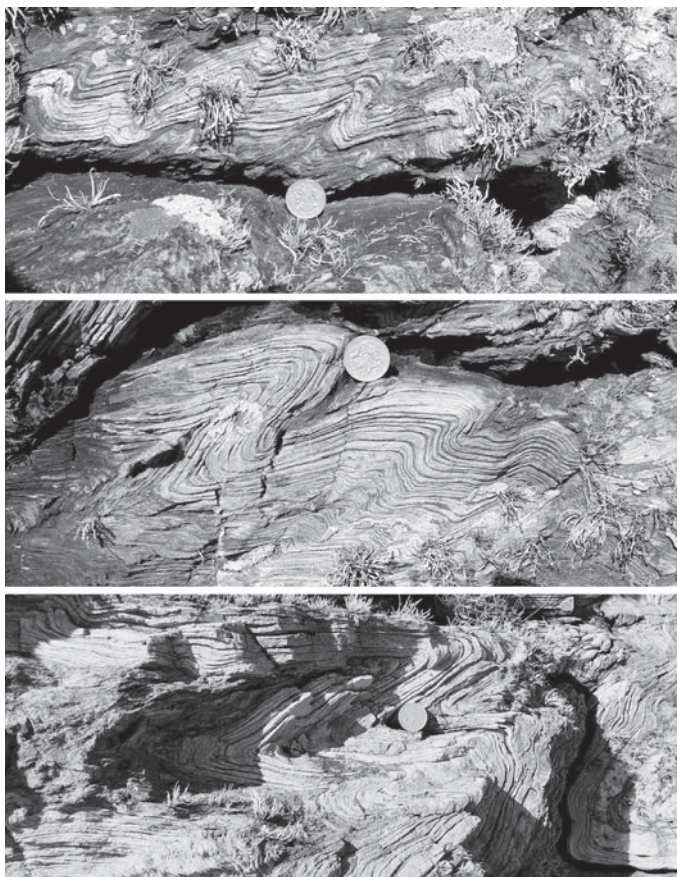


Figure 1.4. Severe folding of metamorphic rock layers (so-called accommodation structures) initiated as buckling owing to compression stresses (Trearddur Bay, Holyhead, N. Wales, UK; the coin in the photos is a pound). (See color plates section.)

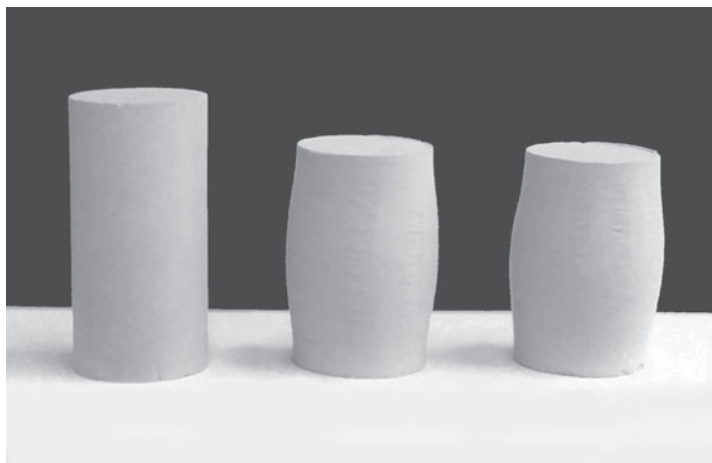


Figure 1.5. Examples of barreling of a 36.5×74.9 -mm cylindrical silty clay (normally consolidated, namely, with an overconsolidation ratio equal to 1) sample (shown intact on the left) tested under undrained triaxial compression. Barreling has been a progressive phenomenon, initiated after a small (near 2%) homogeneous strain (the test was interrupted at an axial strain near 10%). A sample tested with a fixed top is shown in the centre, whereas a free top was used to test the sample visible on the right. No substantial difference between the behaviours of the two specimens was found in the global stress/strain response (reported in Fig. 1.18).

in the (cylindrical and dog-bone-shaped strip) metal specimens pulled in tension in Fig. 1.6.³ While barreling and Euler buckling are examples of diffuse bifurcations, necking is an example of localized bifurcation. Note also that necking is a bifurcation occurring for tensile load.⁴

1.2 Bifurcations in elasticity: The elastic cylinder

Although the behaviour of materials is often inelastic near bifurcation stresses so that, for instance, the necking and barreling shown in Figs. 1.5 and 1.6 typically involve plastic deformation, elasticity remains a useful framework for the analysis of bifurcation.⁵

Some bifurcation thresholds and relative modes of deformation are reported in Fig. 1.7 for uniaxial compression of a cylindrical specimen made up of an elastic incompressible material, with material parameters selected to simulate the behaviour of silicon nitride at high temperature (example taken from Gei et al. 2004 and developed in detail in Chapter 12). The compression is transmitted through contact with two smooth and rigid constraints at the edges. Both the nominal and true

³ Additional (beautiful) examples of plastic bifurcation have been given by Rittel and Roman (1989), Rittel (1990), and Rittel et al. (1991).

⁴ Necking is a *bifurcation occurring for tensile axial loads*, whereas bifurcation of structural elements such as beams, columns and frames is normally believed to be associated with compressive loads. An example reported in Section 1.13.2 will be sufficient to show that buckling of structures subject to tensile dead load can occur for simple mechanical systems (see also Zaccaria et al. 2011).

⁵ Chapters 10 and 11 are devoted to the general theory of bifurcation and instability in elastic and plastic solids (the former section to global and the latter to local conditions), whereas examples of bifurcations for elastic and elastoplastic solids are presented in Sections 12 and 13, respectively.

1.2 Bifurcations in elasticity: The elastic cylinder

7



Figure 1.6. Examples of localization of deformation occurring for tensile loads in low-carbon steel samples. *Top*: Necking is the first mode occurring in the dog-bone-shaped strip shown in the figure. Later, shear banding (with a 45° inclination) develops within the necked zone, which eventually degenerates into a fracture (visible in the photo). *Bottom*: Necking in a cylindrical bar under tension.

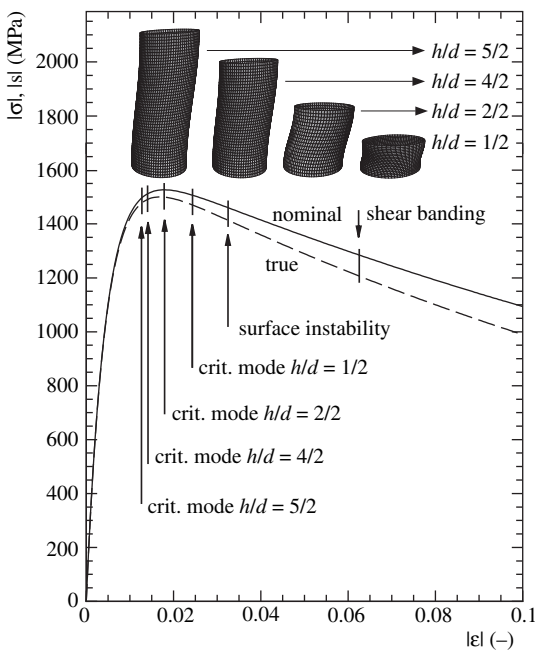


Figure 1.7. Bifurcation thresholds (in terms of true σ and nominal s stress versus axial logarithmic strain) of an elastic, incompressible cylinder uniaxially compressed through smooth and rigid constraints (adapted from Gei et al. 2004). Some modes associated with initial bifurcations for different aspect ratios ($h/d = 1/2, 1, 2, 5/2$) are sketched in the upper part. Note that surface bifurcation (or surface instability) and shear banding are extreme forms of instability, occurring ‘far’ in the softening regime.

stresses are reported (the latter dashed) in the figure versus the (absolute value of) logarithmic strain for homogeneous response. The threshold stresses for the first bifurcations are called ‘critical’ (denoted with ‘crit’) and may occur for different aspect ratios (namely $h/d = 1/2, 1, 2, 5/2$). These are marked on the curves in Fig. 1.7.

The different modes of bifurcation may be triggered by boundary conditions, for instance, if the elastic cylinder represents a specimen in a testing machine, by the specific test geometry, stiffness of the machine, or friction at the contact with the loading plates. For example, a high slenderness will induce a Euler-type bifurcation, whereas friction at the contact between specimen and end supports will favour development of barreling. The example of the elastic cylinder illustrates the great variety of bifurcation mechanisms often observable during mechanical tests.

Two peculiar bifurcation instabilities in Fig. 1.7 will receive a strong attention later, namely, *surface bifurcation* or *surface instability* and *shear banding*.⁶ These instabilities occur at high strain, after other bifurcations, so these represent extreme forms of instabilities.

1.3 Bifurcations in elastoplasticity: The Shanley model

Bifurcation and instability theory is much simpler for elastic materials than for elastoplastic materials. The complication inherent to elastoplastic models, which are dissipative, already can be appreciated by considering the behaviour of the elastoplastic spring shown in Fig. 1.8 on the left. In particular, since during elastoplastic behaviour the response differs from loading (stiffness k_l , the so-called plastic branch of the constitutive equation) to unloading (stiffness k_e , the so-called elastic branch of the constitutive equation), the constitutive equation has to relate *incremental* (instead of finite, as in elasticity) quantities and in an *incrementally non-linear* (*piece-wise linear*) *relation* (instead of an incrementally linear way, as in nonlinear elasticity). The complication introduced by the constitutive equation yields peculiar features for problems of plastic bifurcation and instability that can be illustrated with the simple example of the celebrated Shanley (1947) model for plastic column buckling. The Shanley model is shown in Fig. 1.8 (*centre* and *right*) and consists in a T-shaped rigid rod constrained to move vertically and possibly rotate about the node of the T (see also Hutchinson 1973, 1974). The rigid rod is connected to two elastoplastic springs (behaving as in Fig. 1.8, *left*), subject to a vertical compressive load F (taken positive for compression), which before bifurcation is simply equal to $P/2$. We assume that F is (1) either at yielding, namely, at its maximum value F_{\max} (in the plastic branch of the constitutive equation of the springs; Fig. 1.8, *left*) or (2) is unloading after having reached F_{\max} . Therefore, the two springs obey the following force

⁶ Surface instability is characterized by the fact that the wavelengths of the bifurcation mode may become infinitely small. This is a tendency already visible in Fig. 12.17 of Chapter 12, where modes R , T and U correspond to increasing circumferential and longitudinal wavenumbers (see Fig. 12.18). Subsequent bifurcations involve smaller wavelengths, which approach zero at surface instability, representing an *accumulation point for bifurcation loads*.

1.3 Bifurcations in elastoplasticity: The Shanley model

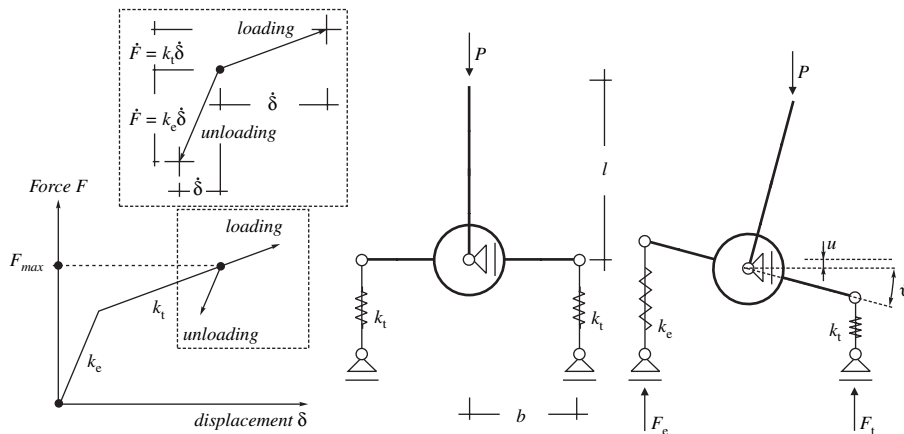


Figure 1.8. *Left:* Force-displacement relation for an elastoplastic spring. *Centre and right:* Shanley model for plastic column buckling. The rigid T-shaped rod has two degrees of freedom $\{u, \theta\}$ and is constrained by two elastoplastic springs, displaying the piecewise-linear force-displacement behaviour shown on the left.

F – displacement δ rate constitutive relation:

1. At yielding: $F = F_{\max} \implies \begin{cases} \dot{F} = k_t \dot{\delta}, & \text{for plastic loading } \dot{F} > 0, \\ \dot{F} = k_e \dot{\delta}, & \text{for elastic unloading } \dot{F} < 0, \end{cases} \quad (1.1)$
2. Within the elastic range: $F < F_{\max} \implies F = k_e \delta.$

where superposed dots denote rates.

Note the incremental non-linearity (more precisely, piecewise linearity) of the constitutive equations, which exhibit two different branches, one for plastic loading and another for elastic unloading (the so-called neutral loading corresponds to $\dot{\delta} = \dot{F} = 0$). This nonlinearity in the rate represents the main complication of elastoplasticity.

It is assumed that the system is loaded until the springs are in the plastic range, without any prior elastic instability. This loading occurs without any rotation and defines the fundamental path, where $F = P/2$. Bifurcations are sought as quasi-static (namely, involving negligible dynamical effects) departures from this configuration, in terms of a rate vertical displacement \dot{u} of the centre of the T-shaped rod and a rate rotation $\dot{\theta}$. Note that we intend with ‘rate’ the derivative with respect to an increasing time-like parameter governing the loading of the system.

Equilibrium written for a configuration displaced a finite amount u and θ is readily obtained as

$$P = F_e + F_t \quad Pl \sin \theta + (F_e - F_t)b \cos \theta = 0, \quad (1.2)$$

with displacements in the springs

$$u_t = u + b \sin \theta \quad u_e = u - b \sin \theta. \quad (1.3)$$

By approximating Eqs. (1.2) and (1.3) for small θ and taking the rates, we obtain the rate equations, holding for a configuration close to the fundamental path

$$\dot{P} = \dot{F}_e + \dot{F}_t \quad (P\theta)' l + (\dot{F}_e - \dot{F}_t)b = 0, \quad (1.4)$$

whereas the rate of displacements in the springs are

$$\dot{u}_t = \dot{u} + b\dot{\theta} \quad \dot{u}_e = \dot{u} - b\dot{\theta}, \quad (1.5)$$

so the constitutive equations of the springs (1.1) allow us to obtain

$$(P\theta)' = -\frac{k_e - k_t}{k_e + k_t} \frac{b}{l} \dot{P} + P_R \dot{\theta} \quad \dot{u} = \frac{\dot{P}}{k_e + k_t} + \frac{k_e - k_t}{k_e + k_t} b \dot{\theta}, \quad (1.6)$$

where

$$P_R = \frac{4(k_e k_t) b^2}{(k_e + k_t) l} > 0, \quad (1.7)$$

is the so-called reduced-modulus load. Equations (1.6) are valid if the appropriate loading/unloading conditions are satisfied. For positive (clockwise) $\dot{\theta}$ and using Eqs. (1.5), these conditions are

$$\dot{u} - b\dot{\theta} < 0, \quad \dot{u} + b\dot{\theta} > 0. \quad (1.8)$$

From Eqs. (1.6) we can observe the following.

- Analysis of bifurcations emanating from the fundamental path, $\theta = 0$, is governed by the equations

$$\frac{k_e - k_t}{k_e + k_t} \frac{b}{l} \dot{P} = (P_R - P) \dot{\theta} \quad \dot{u} = \frac{\dot{P}}{k_e + k_t} + \frac{k_e - k_t}{k_e + k_t} b \dot{\theta}. \quad (1.9)$$

Working Eqs. (1.9) into Eqs. (1.8), we can write the conditions enforcing the satisfaction of loading/unloading constraints in the springs

$$P_T \leq P \leq P_E \quad P_T = \frac{2k_t b^2}{l} \quad P_E = \frac{2k_e b^2}{l}, \quad (1.10)$$

where P_T is the so-called tangent modulus load, whereas P_E is the critical load corresponding to a purely elastic bifurcation.

For a value of the load P belonging to the interval $[P_T, P_E]$, bifurcations are possible because Eqs. (1.9) always admit a non-trivial solution. There are three particular cases of interest: (1) When $P = P_T$, bifurcation occurs as if the two springs were elastic and both are characterized by a stiffness k_t ; moreover, neutral loading (i.e., $\dot{u}_e = 0$) occurs for the unloading spring, which remains ‘frozen’ at bifurcation. (2) When $P = P_R$, bifurcation occurs at a fixed load (i.e., for $\dot{P} = 0$). (3) When $P = P_E$, a purely elastic bifurcation occurs.

- Integration of the rate Eqs. (1.6) is simple if the springs do not change their behaviour. Performing the integration from an initial state where the load is $P_{\text{bif}} \in [P_T, P_E]$ and $\theta = 0$ to a final state in which the load is $P = P_{\text{bif}} + \Delta P$ and the rotation is θ , we obtain

$$\frac{\Delta P + P_{\text{bif}}}{P_R} = \frac{P_{\text{bif}}/P_R(P_E/P_T - 1) + (P_E/P_T + 1)l/b\theta}{(P_E/P_T - 1) + (P_E/P_T + 1)l/b\theta}, \quad (1.11)$$